Interplay of alloying and ordering on the electronic structure of $Ga_xIn_{1-x}P$ alloys

Yong Zhang,[1,*] A. Mascarenhas,[1] and L.-W. Wang[2]
[1]*National Renewable Energy Laboratory, 1617 Cole Boulevard, Golden, Colorado 80401, USA*
[2]*Lawrence Berkeley National Laboratory, Berkeley, California 94720, USA*
(Received 18 August 2008; published 3 December 2008)

In this work, we extend the study of the electronic structure of disordered and ordered $Ga_xIn_{1-x}P$ alloys from the focus of most previous effort, $x\sim0.5$, to the whole composition range, $0<x<1$, using an improved empirical pseudopotential method with a supercell approach that employs a sufficiently large supercell size of ~28 000 atoms—a size needed to realistically model disordered and partially ordered alloys. This study provides insights into the underlying physics of the alloy system in two important phases—disordered and CuPt ordered—and the interplay of alloying and ordering effects. It also offers much-needed guidance for the optimal use of ordering phenomenon in a range of applications including telecommunications, photovoltaics, and solid-state lighting. Critical-point energies, interband transition matrix elements, and optical anisotropy are calculated for both the disordered and ordered phases. The deviation of the wave function of an alloy state from that of a virtual-crystal state is analyzed using a spectral function. The implications of such deviation are examined explicitly for the above-mentioned properties. Unusual ordering effects are revealed in the indirect-band-gap composition region of the alloy. The connection and distinction between the ordered and disordered structures are discussed. An often-used perturbation theory, known as "a quasicubic model," is found to be reasonably accurate for predicting the anisotropy of the interband transition but inadequate for predicting the intensity variation with varying order parameter.

DOI: 10.1103/PhysRevB.78.235202 PACS number(s): 71.20.Nr, 71.23.An

I. INTRODUCTION

$Ga_xIn_{1-x}P$ is one of the most important semiconductor alloy systems for applications in telecommunications (heterostructure bipolar transistors), photovoltaics (multijunction solar cells), and solid-state lighting (red light-emitting diodes). Even though this alloy system has been studied extensively both experimentally and theoretically since the early 1970s,[1] its electronic structure is accurately known only for x near 0.5.[2] This much is known because $x\sim0.5$ is the lattice-matching composition for the alloy with GaAs and thus has been the preferred and widely used composition in practical applications until very recently. For instance, the critical composition of the direct-to-indirect transition x_c still remains uncertain from extensive early studies. Experimentally, it ranges from 0.63 to 0.74 (Refs. 3 and 4) and is described as either Γ-to-X (Ref. 3) or Γ-to-L (Refs. 4 and 5); theoretically, it ranges from $x_{\Gamma\text{-}X}=0.695$ of a tight-binding calculation (Ref. 6) to 0.74 of a model analysis.[3] In addition, the general belief seems to be that only one direct-to-indirect transition point exists from Γ to X but both experimental and theoretical studies have also suggested a two-crossover scenario: Γ-L followed by Γ-X.[1,4,5,7]

A very recent breakthrough in multijunction solar cell technology indicates that the use of $Ga_xIn_{1-x}P$ with x significantly away from the lattice-matched composition can substantially increase solar cell efficiency.[8] For solid-state lighting, it remains uncertain whether $(Al_yGa_{1-y})_xIn_{1-x}P$ could provide viable options to fill the "red gap" (615–625 nm) and "green gap" (530–570 nm) for "ultraefficient" (>70%) white-light applications.[9] Furthermore, $Ga_xIn_{1-x}P$ alloys, when grown by metal organic chemical vapor deposition, are often found to exhibit spontaneous CuPt ordering (i.e., the formation of a monolayer superlattice along one of the zinc-blende [111] axes),[10] which not only provides an additional variable order parameter η for tuning the electronic structure (Refs. 11 and 12) but also offers the possibility of mitigating the undesirable alloy scattering.[13] Because the ordering may substantially reduce the band-gap energy (by >100 meV at $x\sim0.5$), the ordering-induced band-gap shift has to be considered in the device design.[8] However, accurate information about the ordering effects on the electronic structure is available only for $x\sim0.5$.[2] It has been suggested that an interpolation relation, the so-called η^2 rule, could be used to obtain the material property P through $P(x,\eta)=P(x,0)+\eta^2[P(0.5,1)-P(0.5,0)]$,[14] but its accuracy has not been seriously tested either theoretically or experimentally for $x\neq0.5$. For $x=0.5$, it has been shown that the leading η^2 term is generally inadequate.[2] Nevertheless, the existence of CuPt ordering in $Ga_{0.7}In_{0.3}P$ has been reported.[15] Therefore, accurate knowledge of both the electronic structure of the $Ga_xIn_{1-x}P$ alloy and the effects of ordering on the whole composition range is critically important to enable exploring the full potential of this alloy system for the above-mentioned energy applications.

We have recently performed a systematic investigation of the basic electronic structure of this alloy system in the disordered or random phase for $0<x<1$.[16] In this work, we further study the interplay of alloying and ordering effects on the electronic structure of the alloys.

The band-gap reduction observed in CuPt-ordered $Ga_{0.5}In_{0.5}P$ has been qualitatively understood as a result of the repulsion between the folded L and Γ points, which occurs predominantly in the conduction band (CB).[17] The effect on the valence band (VB) has indeed been shown to be relatively small.[18] Besides the ordering-induced band-gap reduction, ordering is also expected to change the interband optical transitions. However, previous efforts have focused largely on optical anisotropy, including various spectroscopic

properties associated with interband transition[11,12] that results from the symmetry-lowering effect of ordering. Little attention has been paid to the ordering-induced change in the transition intensity. Essentially, for the optical transition near the fundamental band gap, the ordering effects on the VB were treated by applying a perturbation method,[11,12] whereas the CB was assumed unchanged despite that Γ-L coupling is regularly mentioned as the major source of the observed band-gap reduction. It has been proposed that the CuPt ordering can be used to convert an indirect-gap semiconductor alloy into a direct gap. For example, although both $GaP_{0.5}As_{0.5}$ and $Ga_{0.5}Al_{0.5}As$ have indirect-band gaps with an X-like conduction-band edge, the folded L-like state can, in principle, repel the Γ-like state downward so it becomes lower than the X-like state.[19,20] The same mechanism has been used to explain the direct-gap behavior of CuPt-ordered $(Al_{0.5}Ga_{0.5})_{0.51}In_{0.49}P$, which is generally believed to be an indirect-gap alloy when it is disordered.[21] This quaternary alloy has a band gap near 2.3 eV at 15 K, which represents a substantial increase from that of $\sim$2.0 eV for $Ga_{0.5}In_{0.5}P$ but at the cost of introducing the fourth element along with various undesirable effects. Note that the Γ-L repulsion model implicitly assumes the existence of two states that are dominated by Γ and L components, respectively. However, as indicated recently,[16] it may not always be possible to associate an alloy state with a well-defined k component, which makes it very interesting to see *how* ordering manifests itself in the electronic structure change and *if* the Γ-L repulsion scheme remains meaningful. To extend our understanding of ordering to the whole composition range and address the issues mentioned above, in this work we (1) calculate CuPt-ordering-induced shifts in critical energies, (2) analyze the impact of ordering on the direct-indirect character of the band-edge state, (3) explicitly evaluate interband dipole transition matrix elements between the CB and VB as a function of alloy composition, with and without CuPt ordering, and (4) explore the possibility of increasing the band gap within the ternary system $Ga_xIn_{1-x}P$, while keeping the nature of the interband transition quasidirect, through the interplay of varying composition and by introducing ordering.

II. COMPUTATION AND ANALYSIS METHODS

The same empirical pseudopotential method (EPM) used previously[2,16,18,22] is applied in this work. The (reciprocal-space) empirical pseudopotential takes the form of $v(q,\boldsymbol{\varepsilon}) = v(q,0)[1+a_s\mathrm{Tr}(\boldsymbol{\varepsilon})]$, where $v(q,0)$ is the value at equilibrium lattice constant and $\mathrm{Tr}(\boldsymbol{\varepsilon})$ is the trace of the local strain (approximated by the relative change of the tetrahedron volume).[23] The extra term associated with strain represents a significant improvement versus the conventional EPM, which typically adopts the same empirical pseudopotentials for the whole composition range for the alloy system of interest. This modification not only imposes a constraint on the pseudopotential when fitting the material properties of the binaries but also allows the pseudopotential to be adjusted for the local bond length, which might be different from that in the bulk. It is worth pointing out that because the strain correction is only to the linear term, it might not be adequate for an alloy system with a large lattice mismatch (e.g., $GaP_{1-x}N_x$ with $\sim$18% mismatch between the binaries).[24] Because the pseudopotentials for the common anion P are fit separately for GaP and InP and thus nonidentical, the P pseudopotential is taken as a weighted average in a combined system according to the number of Ga and In atoms on the four nearest-neighbor cation sites to account for the difference in the local chemical environment.[23] The strain term is set to zero for the common anion P pseudopotentials. The pseudopotentials are obtained by fitting to experimentally determined or theoretically calculated electronic properties at their equilibrium conditions. These properties include energies, deformation potentials, effective masses at different critical points, and valence-band offsets. The pseudopotentials can reproduce very well for not only the binary band structures but also for the alloy band structure at $x\sim0.5$ with varying degrees of ordering.[2,18] The pseudopotential also contains a nonlocal spin-orbit interaction component. A plane-wave basis is used to expand the electronic wave function, with a kinetic-energy cutoff of 7 Ry.

A supercell approach is used to model the random and ordered alloys. The CuPt-ordered alloy is a [111] monolayer superlattice that can be defined as $Ga_{x+\eta/2}In_{1-x-\eta/2}P/Ga_{x-\eta/2}In_{1-x+\eta/2}P$, where η is the order parameter that has a maximum value $\eta_{\max}(x)$ equal to the smaller values of $2x$ and $2(1-x)$. In this work, only two extreme situations, $\eta=0$ and $\eta=\eta_{\max}(x)$, are considered. At $x=0.5$, the fully ordered structure is simply a superlattice of alternating monolayers of GaP and InP. For $x>0.5$ or <0.5 with $\eta=\eta_{\max}$, it alternates between a pure GaP or InP monolayer and a $Ga_{x'}In_{1-x'}P$ monolayer with $x'=(2x-1)$ or $(2x)$. For convenience in studying the CuPt ordering, an orthorhombic supercell is built with three cell vectors, $\mathbf{a}_1$, $\mathbf{a}_2$, and $\mathbf{a}_3$, along the $x'\sim[11\bar{2}]$, $y'\sim[\bar{1}10]$, and $z'\sim[111]$ directions of the zinc-blende (ZB) crystal, respectively.[2] The lattice constant $a(x)$ is assumed to obey Vegard's rule with $a_{\mathrm{GaP}}=5.447$ Å and $a_{\mathrm{InP}}=5.8658$ Å for both disordered and ordered structures. For the CuPt-ordered structure, it is possible to have a cubic lattice when the material is grown epitaxially on a substrate with the same lattice constant. A supercell containing 27 648 atoms, with $a_1=12\sqrt{3/2}a$, $a_2=12\sqrt{2}a$, and $a_3=8\sqrt{3}a$, is used, which ensures that the band gaps will converge to within a few meV.[2] A valence force field method is applied to relax all the atoms within the supercell to minimize the strain energy.[25] Virtual-crystal calculations are also performed using the same supercell sizes, with the pseudopotential given by $v(q,\boldsymbol{\varepsilon})=xv^{\mathrm{GaP}}(q,\boldsymbol{\varepsilon})+(1-x)v^{\mathrm{InP}}(q,\boldsymbol{\varepsilon})$. To solve the Schrodinger equation for the large systems involved, a folded spectrum method is used,[26] which allows solving for only the states near the band edge within an energy range of interest (e.g., including Γ, L, and X points).

A virtual-crystal approximation (VCA) has often been used as the zero-order approximation for the real alloy[27,28] even with the presence of long- or short-range orderings.[29,30] If we denote $[\phi_n(\mathbf{k},\mathbf{r}),E_{n\mathbf{k}}]$ as the VCA solutions of the alloy system with band index n and wave vector $\mathbf{k}$ defined in the ZB Brillouin zone (BZ), an alloy eigenstate $\varphi_i(\mathbf{r})$ with energy E can then be expanded to the Bloch states $[\phi_n(\mathbf{k},\mathbf{r})]$.

The degree to which the alloy state resembles the Bloch state can then be described quantitatively by a **k**-space projection function[31]

$$P_i(k) = \sum_n |\langle \varphi_i(r) | \varphi_n(k,r) \rangle|^2. \quad (1)$$

However, to evaluate $P_i(\mathbf{k})$, we do not actually need to calculate explicitly $[\phi_n(\mathbf{k},\mathbf{r}), E_{n\mathbf{k}}]$ or to define exactly what the VCA is. Instead, a reciprocal-space analysis can be used to calculate $P_i(k)$ directly. If $\varphi_i(\mathbf{r})$ is dominated by one-component $\mathbf{k}_0$ with a limiting value $P_i(\mathbf{k}_0)=1$, we may consider this state to be primarily derived from the $\mathbf{k}_0$ Bloch state of the virtual crystal and the spectrum of $P_i(\mathbf{k})$ reveals how many other $(\mathbf{k} \neq \mathbf{k}_0)$ Bloch states the $\mathbf{k}_0$ state is coupled to by the potential fluctuation. One can alternatively define a spectral function as[32,33]

$$A(k_0,E) = \sum_i P_i(k_0)\,\delta(E - E_i). \quad (2)$$

$A(\mathbf{k}_0,E)$ instead indicates to what extent the $\mathbf{k}_0$ Bloch state is mixed into other states of different energies and is a pertinent property for a real alloy. In the supercell approach, we typically calculate just enough eigenstates (at $k=0$ of the supercell) to include all the folded states from the Γ, L, and X points of the ZB BZ and then we evaluate $P_i(k)$ for each of them. The convergence of $P_i(\mathbf{k})$ with increasing the supercell size is somewhat slower than the energy levels, especially for the high-lying states, for the required accuracies: a few meV for the energy level and a few percent for $P_i(\mathbf{k})$. For the ordered structures, we use only the 27 648-atom supercell. For the random structures, we also use smaller supercells (3456 atoms) for calculating critical points far away from the band edge.[16] Because the numbers of folded k points that are available for coupling by the perturbation potential depend on the size, as well as the orientation, of the supercell, the obtained $P_i(\mathbf{k})$ should be considered as the upper bound of the ultimate value of an infinite crystal.

An interband dipole transition matrix element is important for evaluating the strength of the interband optical transition for the material. It provides complementary information to the analysis of the individual CB or VB states given by $P_i(\mathbf{k})$ and $A(\mathbf{k}_0,E)$. We thus also calculate the transition intensity, the square of the transition matrix element, for both random and ordered phases throughout the entire composition range. The transition intensity is defined as

$$I_{\mathrm{CV}}(\mathbf{e}) = |M_{\mathrm{CV}}(\mathbf{e})|^2 = \sum_{i,j} \langle \varphi_i | \mathbf{e} \cdot \mathbf{p} | \varphi_j \rangle^2, \quad (3)$$

where φ_i and φ_j are the CB and VB states, respectively, at $\mathbf{k}=0$, the summation is performed over nearly degenerate states (e.g., the three nearly degenerate X-like states in the CB and two nearly degenerate topmost VB states for a random alloy), **e** stands for the unit vector of the light polarization, and **p** is the momentum operator.

III. RESULTS AND DISCUSSIONS

A. Energy levels and wave functions of the critical points

Figure 1 summarizes the energy levels of the three major critical points (Γ, L, and X) and corresponding band gaps with respect to the valence-band maximum (VBM) of InP for $Ga_xIn_{1-x}P$ in both random and CuPt-ordered phases. The numerical results for the random phase can be fitted very well with the following well-known equation:

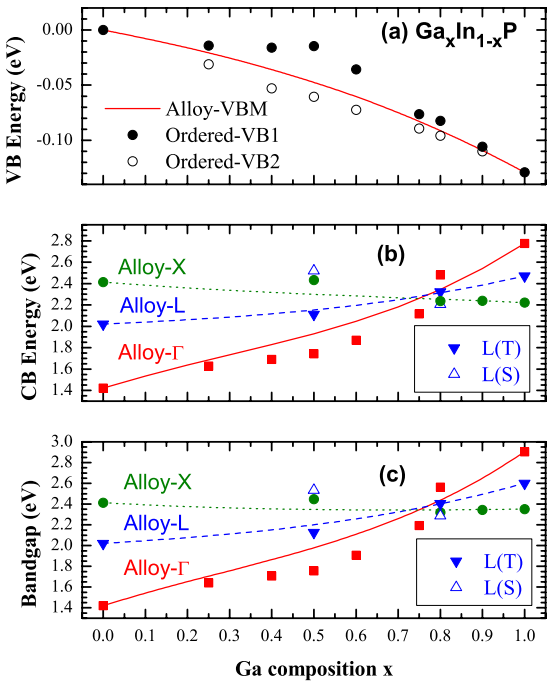

FIG. 1. (Color online) Energy levels of the major critical points in random and maximally ordered $Ga_xIn_{1-x}P$. Lines represent the random alloy and symbols the ordered phase (a) for the valence band, (b) for the conduction band, and (c) for the band gaps. The energy reference in (a) and (b) is the valence-band maximum of InP. T stands for triplet and S for singlet.

$$E(x) = E(0) + [E(1) - E(0)]x - b(x)x(1-x), \quad (4)$$

where $b(x)=b_0+b_1x$. The fitting parameters are summarized in Table I. Figure 1(a) is for the VB energies at the Γ point. The CuPt ordering has caused a splitting of the nearly degenerate VBM states in the random phase (resembling the degenerate Γ_8 and Γ_7 states in a ZB structure, shown by the curve of averaging over the two topmost VB states). The splitting is maximized at $x \sim 0.5$, at which the maximum or-

TABLE I. Fitting parameters for used with Eq. (4) (in electron volts).

	$E(0)$	$E(1)$-$E(0)$	b_0	b_1
$E_{\mathrm{CB}\Gamma}$	1.421	1.353	0.139	1.051
$E_{\mathrm{CB}L}$	2.021	0.451	0.282	0.187
$E_{\mathrm{CB}X}$	2.412	−0.190	0.109	−0.079
E_{VBM}	0	−0.129	−0.056	−0.026
$E_{g\Gamma}$	1.421	1.482	0.195	1.078
E_{gL}	2.021	0.580	0.338	0.213
E_{gX}	2.412	−0.060	0.165	−0.052

der parameter $\eta_{max}(x)$ also maximizes to $\eta_{max}(0.5)=1$, corresponding to an ideal monolayer superlattice of GaP/InP. At the same time, the ordering effect raises the VBM relative to the random alloy although by a relatively small amount ($\sim$33 meV at $x=0.5$). Figure 1(b) shows the CB energy levels of the Γ-, L-, and X-like states in the random and ordered phases. For the ordered phase, the higher critical points are obtained only for two compositions: $x=0.5$ and 0.8. The association of an energy level with a critical point is determined by analyzing the k-space projection of the alloy wave function using Eq. (1) and/or Eq. (2). For the random phase, our calculation shows only one direct-to-indirect crossing point, i.e., $x_{\Gamma\text{-}X}=0.75$. For the ordered phase, the ordering-induced CB lowering maximizes at $x\sim0.5$ with $\delta E_\Gamma=-188$ meV. However, it remains fairly large with $\delta E_\Gamma=-133$ meV, even for $x=0.75$ at which $\eta_{max}(0.75)$ is only 0.5. In contrast, for $x=0.25$ with the same $\eta_{max}(0.25)=0.5$, the CB lowering is somewhat smaller $\delta E_\Gamma=-58$ meV. The lowering of the conduction-band minimum (CBM) in the CuPt-ordered alloys has been explained by an intuitive two-level model:[17] the repulsion between the alloy CBM and L point, which occurs because the CuPt ordering makes the L point along the ordering direction fold into the Γ point in the ordered structure. This simple model can indeed account for the difference between $x=0.25$ and 0.75, both with $\eta_{max}=0.5$, as being due to the difference in the Γ-L separation. For $x=0.8$, because the alloy Γ-like state is above the L-like state, the CBM of the ordered structure should be L like based on the consideration of Γ-L repulsion. However, in this case, it is ambiguous or not practically meaningful to distinguish this CBM state between Γ like and L like because it has a comparable amount of Γ and L components as will be further illustrated later. A direct consequence of the Γ-L coupling is a splitting of the fourfold nearly degenerate L-like states in the random phase: a splitting between the [111] valley (coinciding with the ordering direction) and the other three [111] valleys. As shown in Fig. 1(b), at $x=0.5$, the singlet L-derived state, $L(S)$, has been pushed up somewhat more than the Γ-like state being pushed down. There is further coupling among the three remaining L valleys, $L(T)$, and the three X valleys because they happen to fold into the same k point of the new BZ of the ordered phase,[34] which leads to both sets of states shifting from their alloy positions in the opposite directions, as shown clearly in Fig. 1(b) for $x=0.5$. In this figure, the CBM of the ordered-phase switches from Γ like to X like at a composition beyond $x=0.8$ (approximately at $x\sim0.82$). Figure 1(c) plots the corresponding band gaps for the ordered phase compared to those of three critical points for the random phase. As is evident, the η^2 rule[14] is quite inaccurate for either the CB lowering or the band-gap reduction: $\delta E_g(x=0.25,\eta=0.5)=-63$ meV vs $\delta E_g(x=0.75,\eta=0.5)=-151$ meV. The reason is also quite obvious. The η^2 rule suggests that the ordering-induced band-structure change depends only on the change at $x=0.5$ with $\eta=1$. However, as shown above, the ordering-induced band-structure change depends sensitively on the band structure at a specific composition, for instance, the Γ-L separation.

Figure 2 shows the evolution of the energy levels from the alloy phase, either in the VCA or as a random alloy, to the

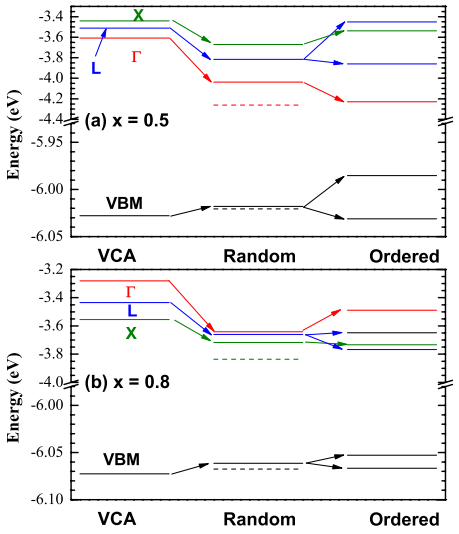

FIG. 2. (Color online) Energy levels of $Ga_xIn_{1-x}P$ alloys in a "virtual-crystal" approximation, fully relaxed random phase, and CuPt-ordered phase. The dashed lines in the middle section represent the unrelaxed random phase (a) for $x=0.50$ and (b) for $x=0.80$.

CuPt-ordered phase for two compositions of particular interest: $x=0.5$ and $x=0.8$. We notice that as shown in Fig. 1(b) for the ordered phase with $x=0.5$, the upward shift of the singlet L-like state is much larger than the downward shift of the Γ-like state from the respective states in the random alloy phase. However, as shown in Fig. 2(a), when compared to the VCA results, the downward shift of the Γ-like state is instead much larger than the upward shift of the singlet L-like state. Therefore, it is ambiguous to use which one of them as the reference for quantitatively interpreting the ordering result using the Γ-L repulsion scheme, which indicates the qualitative nature of this simple model. By explicitly calculating their wave-function projections for $x=0.5$, we find that the Γ-like band edge and the L-like singlet contain only L and Γ components of the ZB BZ, with $P_\Gamma=0.655$ and $P_L=0.345$ for the Γ-like band edge and $P_\Gamma=0.438$ and $P_L=0.562$ for the L-like singlet. Because the total Γ component of the two states exceeds 1, these results indicate that the ordering does not simply induce coupling within the CB band but also involves other bands. Similarly, we also notice that for $x=0.5$, the shift of the X-like state is substantially different from that of the triplet L-like state when compared to either the VCA or random-alloy states, as shown in Figs. 1(b) and 2(a). It is more interesting to examine $x=0.8$, for which we have previously shown that the Γ-like state can barely be viewed as Γ like, because of P_Γ being as small as 0.092.[16] Despite the fact that this Γ-like state is above the L like in the alloy phase, we find that in the ordered phase, the CBM exhibits the largest Γ component of $P_\Gamma=0.411$ among all the states within $\sim$0.3 eV of the CBM but with $P_L=0.536$ (mostly the [111] valley). The other state with the second-largest Γ component as well as [111] L component lies at 275 meV above the CBM but with both Γ and L components being rather small: $P_\Gamma=0.020$ and $P_L=0.017$. In fact, they are smaller than those for the random alloy. Therefore, strictly speaking for this case, neither the

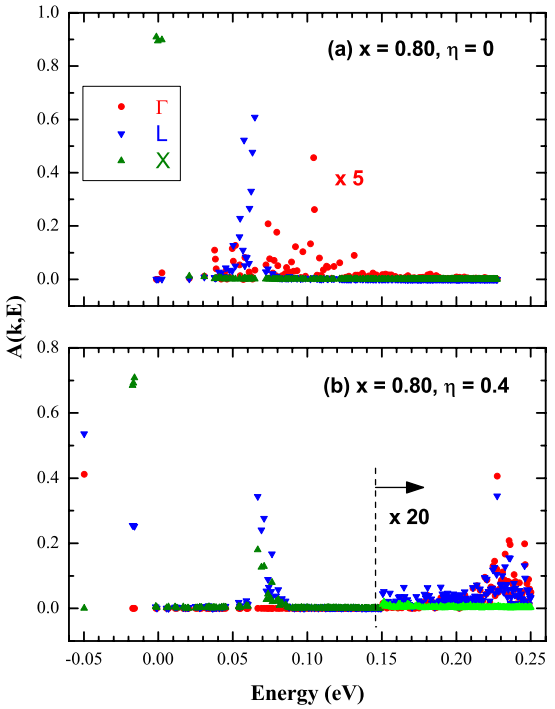

FIG. 3. (Color online) Spectral functions of $Ga_{0.8}In_{0.2}P$ for critical points of $\mathbf{k}_0=\mathbf{k}_\Gamma$, $\mathbf{k}_L$, and $\mathbf{k}_X$ (a) for the random alloy and (b) for the maximally ordered structure. The energy reference is the conduction-band minimum of the random alloy.

Γ-like nor the singlet *L*-like state is well defined. The other three *L*-like states also have only moderate *L* components ($P_L \sim 0.24-0.34$), less than in the random alloy ($P_L \sim 0.33-0.61$). Figure 3 depicts the spectral functions for $x=0.8$ in the random and CuPt-ordered phases. Note that for the random-alloy phase, $A(\Gamma,E)$ has been found to spread over a large spectral range of more than 230 meV, with a peak amplitude of <0.1. The ordering has effectively concentrated a major part of the Γ component into the new band-edge state, as shown in Fig. 3. We would like to emphasize that because of the complexity of the alloy states and the poor accuracy of the VCA in general, using either the random phase or VCA alloy as the reference for understanding or treating the ordering effect might not always be appropriate.

One might assume that an alloy state with $P(\mathbf{k}_0)$ close to 1 should behave very similarly to a VCA state of $\mathbf{k}_0$. Here we offer a detailed examination of the relationship between an alloy state and a VCA state for both random and ordered phases, illustrated with analyses for one composition: $x=0.5$. Applying Eq. (1), we find that the CBM of the random structure has $P_\Gamma=0.864$ compared to the ideal VCA value $P_\Gamma=1$. This value represents the total Γ component (i.e., summed over all the bands) of an unspecified VCA basis. When using a particular VCA basis defined by the VCA pseudopotentials described in Sec. II, we find that the CBM is 430 meV higher than that of the random alloy. The projection between the alloy and VCA state is calculated to be $P_{\mathrm{CB}}(\Gamma)=|\langle\varphi^{\mathrm{alloy}}_{\mathrm{CBM}}(r)|\phi^{\mathrm{VCA}}_{\mathrm{CBM}}(\Gamma,r)\rangle|^2=0.842$, indicating that the alloy CBM is indeed derived primarily from the CBM of the VCA. However, the seemingly small deviation (15.8%) from the VCA state is significant enough to yield the large energy shift of 430 meV and a significant reduction in the interband transition intensity by 26% (see Sec. III B). It is interesting to note that the CBM of an unrelaxed random alloy is lower than the relaxed one by 222 meV, as shown in Fig. 2(a). It is expected that the first-order perturbation to the VCA state should be identically zero[6] if the random alloy is unrelaxed and without any nonlocal effect. Indeed, we have verified $\delta E=\langle\phi^{\mathrm{VCA}}(k,r)|V^{\mathrm{alloy}}-V^{\mathrm{VCA}}|\phi^{\mathrm{VCA}}(k,r)\rangle=0$ for the unrelaxed random structure, where V^{alloy} and V^{VCA} are the potential energies of the supercells. However, for the relaxed structure, we find $\delta E=+113$ meV (using above formula) for the CBM. The positive shift can be understood as a result of moving the atoms in the relaxed structure away from the ideal ZB positions. Note that because of the atomic displacements caused by lattice relaxation, the VCA basis cannot serve as the appropriate zero-order approximation for perturbation calculations of the relaxed alloy, for example, by calculating the alloy scattering matrix element, $\langle\phi^{\mathrm{VCA}}(k',r)|V^{\mathrm{alloy}}-V^{\mathrm{VCA}}|\phi^{\mathrm{VCA}}(k,r)\rangle$, which is a standard practice in the literature for studying electron transport in an alloy. A similar situation is encountered in a $\mathbf{k}\cdot\mathbf{p}$ theory treating the effect of either uniform or nonuniform strain, in which a coordinate transform is needed to make the perturbation procedure appropriate.[35,36] For the ordered structure, we find the single-band contribution to be $P_{\mathrm{CB}}(\Gamma)=0.588$, compared to $P_\Gamma=0.655$ for all bands, which is a clear indication that the ordering has caused significantly more interband mixings than alloying. For instance, the coupling to the VB, $P_{\mathrm{VB}}(\Gamma)$, is only 0.007 for the random structure, whereas it increases to 0.029 for the ordered structure.

There is an interesting implication of the Γ-*L* coupling in the ordered phase. The *L*-like singlet typically acquires a significant Γ component as a result of such coupling. It has recently been shown that the N-doping-induced intraband mixing in $GaAs_{1-x}N_x$ results in an above-band gap or resonant-emission band. This emission is due to radiative recombination between the perturbed GaAs host states near the CB *L* point and the VBM under the condition of high excitation density (e.g., using *μ-PL*).[37] It might be possible to detect similar emission between the *L*-like singlet and the VBM in the ordered $Ga_xIn_{1-x}P$ alloys. If such a measurement is indeed successful, the result will provide additional insight into the ordering effect on the *L* point, complementary to the reported ordering-induced splitting for the E_1 transition,[38] and therefore useful experimentally derived information for the effect of ordering on the valence band near the *L* point.

B. Interband dipole transition matrix elements

While the *k*-space projection provides valuable insight for the origin of an individual CB or VB state in the random or ordered phase by relating it to the VCA alloy, the interband transition matrix element provides more direct information for visualizing the consequences of either alloying or ordering on optical properties such as interband absorption or radiative recombination. Figure 4 shows the calculated transition intensities for $Ga_xIn_{1-x}P$ in both the random and ordered phases. For the random alloy, the contribution of the two

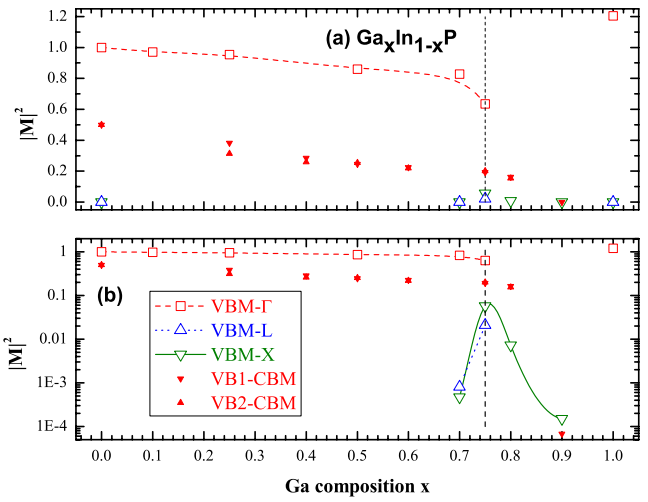

FIG. 4. (Color online) Calculated transition intensities for the interband dipole transition in random (open symbols) and maximally ordered (solid symbols) $Ga_xIn_{1-x}P$ alloys (a) in linear scale and (b) in logarithmic scale. The results are normalized to that for the direct transition in InP.

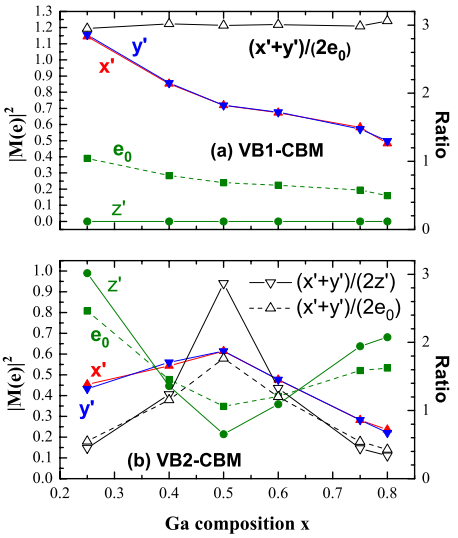

FIG. 5. (Color online) Interband transition intensities for four major polarizations (see text for definitions) and the relevant anisotropy ratios (a) for the transition between the highest valence band and the conduction-band minimum and (b) for the second valence band.

nearly degenerate topmost VB states are combined but for the ordered phase, the transitions from two split VB states [in Fig. 1(a)] are shown separately. The results shown in Fig. 4 are the averages of the three orthogonal polarizations (x', y', and z' for the ordered phase). The optical anisotropy of the CuPt-ordered structure will be discussed later. For the random alloy, $|M|^2$ decreases monotonically from $x=0$ to $x=0.75$ (the direct-gap composition region): for instance, $|M|^2=0.86$ at $x=0.50$ and 0.64 at $x=0.75$. The ordered phase follows a similar trend but extends the quasidirect transition to at least $x=0.80$ at which $|M|^2=0.163$ and 0.154, respectively, from the first and second VB states to CBM and the sum of them is 37% of that of the disordered phase at $x=0.5$. In the direct-gap composition region of the random alloy, the CuPt ordering has an undesirable effect, a reduction in the transition intensity compared to the disordered phase due primarily to the Γ-L mixing, which is expected to affect the light absorption strength and radiative recombination rate. However, the ordered phase should, in principle, have significantly improved carrier mobility and thus conductivity, which is due to the reduction in the alloy fluctuation-induced carrier scattering. The hint for such improvement can be found in the reported major reduction in the excitonic line width or alloy fluctuation as a result of spontaneous ordering in $Ga_{0.52}In_{0.48}P$ alloys.[13] Note that although the reduction in the transition matrix element has been explained as the result of Γ-L mixing, which is meaningful only when we insist on using the alloy phase as the reference, the calculation is done for a direct transition at the Γ point of the new crystal structure (a perfect crystal for $x=0.5$ and $\eta=1$). The result perhaps suggests a general tendency for a crystalline material with the same chemical composition but reduced symmetry to have lower interband transition intensity.

Weak zero-phonon light absorption and emission have been reported in the indirect-band-gap region of $Ga_xIn_{1-x}P$ as well as other semiconductor alloys, which has been explained as a result of the potential fluctuation-induced intervalley coupling that generates a finite Γ component in the wave function of an otherwise indirect-band-edge state.[39] The intervalley coupling is also important for understanding phonon sidebands of the photoluminescence in an indirect-gap semiconductor alloy.[40] The standard theory, based on a perturbative consideration, is that $|M|^2 \propto x(1-x)/\Delta^2$, where $\Delta(x)=E_\Gamma(x)-E_X(x)$ for the X-like indirect-band edge.[39] Such a theory is of little practical use for any quantitative analysis. The theory implicitly assumes that VCA states are the reference. For an alloy with strong lattice relaxation, the VCA is not at all appropriate as a zero-order approximation as already discussed above. However, explicit calculations of the transition intensity for such alloys are not readily available in the literature. Here we have calculated the transition matrix elements for the X- and L-like states near the direct-to-indirect transition point $x_{\Gamma\text{-}X} \sim 0.75$, as shown in Fig. 4. At $x=0.75$, $|M|^2=0.057$ for the X-like state and 0.021 for the L-like state; at $x=0.80$, $|M|^2=0.007$ for the X-like state. Because the absorption coefficient of a direct-gap material is typically more than 10^4 times stronger than that of an indirect gap, even for $|M|^2=0.01$, the absorption coefficient of an indirect alloy could reach roughly 10^2 of a pure indirect-band-gap material, which semiquantitatively accounts for the observation of the zero-phonon absorption and emission in semiconductor alloys such as $Ga_xIn_{1-x}P$.

We now discuss the optical anisotropy caused by CuPt ordering in $Ga_xIn_{1-x}P$ alloys. Figure 5 shows the $|M(\mathbf{e})|^2$ for light polarized in three directions, x', y', and z', as well as the anisotropy ratios; x' and y' are symmetrically equivalent if the structure is fully ordered (only possible at $x=0.5$). The small difference between x' and y' for $x \neq 0.5$ is due to the use of a single supercell that exhibits some randomness in one sublattice. The matrix elements shown in Fig. 5 are normalized to one-half of the average value at $x=0$ (because of

the difference in the degeneracy of the VBM). Figure 5(a) shows the $|M|^2$ for the transitions between the VB1 (i.e., VBM) and CBM. For the polarization perpendicular to the ordering axis (i.e., x' or y', indicated as $x'-y'$ hereafter), the transition is dipole allowed, whereas it is dipole forbidden for the parallel or z' polarization. The reduction in the transition intensity with increasing alloy composition x for the $x'-y'$ polarization is due primarily to the reduction in the Γ component in the CBM wave function as a result of ordering-induced Γ-L mixing. Another useful polarization included in Fig. 5(a) is $\mathbf{e}_0 \sim [110]$, which is an orthogonal direction to y' in the typically adopted growth plane (001). In an often-used perturbation treatment for CuPt ordering,[11,12,41] essentially the quasicubic model proposed by Hopfield,[42] VB1 is treated as a p-like state $|J,m_{z'}\rangle=|3/2,\pm 3/2\rangle$, which gives rise to an anisotropy ratio of 3 between the $x'-y'$ and e_0 polarization. The actual calculated values are within a few percentage points of those based on this simple theory, as shown in Fig. 5(a) (right axis). Even though the perturbation theory is able to yield nearly the same optical anisotropy as the current atomistic calculation, it is difficult to account for the change in the CB wave function and, thus, the transition intensity as a function of x and η. In addition, the residual randomness for $x \neq 0.5$ makes the forbidden z' polarization weakly allowed: the transition intensity is $\sim 10^{-4}$ of the $x'-y'$ polarization. Figure 5(b) shows the transition intensities between the VB2 (the second VB state) and CBM. In the perturbation treatment, this state is derived from $|J,m_{z'}\rangle=|3/2,\pm 1/2\rangle$ but coupled with the spin-orbit split-off band, $|J,m_{z'}\rangle=|1/2,\pm 1/2\rangle$, as a result of the ordering-induced crystal-field splitting. Without ordering, the intensity ratio between the $x'-y'$ and z' polarization is 1 for $|J,m_{z'}\rangle=|3/2,\pm 1/2\rangle$. The ordering-induced coupling with the spin-orbit split-off band, which is strongest at $x=0.5$, tends to enhance the $x'-y'$ polarization. The results shown in Fig. 5(b) reflect the combined effects of varying the CBM Γ component and magnitude of the crystal-field splitting. For the anisotropy ratio between the $x'-y'$ and e_0 polarizations, again the perturbation theory is reasonably accurate: for $x=0.25$, 0.5, and 0.75 with $\eta=\eta_{\max}$, the perturbation theory yields,[41] respectively, 0.597, 1.84, and 0.482, compared to 0.549, 1.77, and 0.543 of the actually calculated values shown in Fig. 5(b).

C. Electronic structure engineering by the interplay of alloy and ordering

The effects of ordering in $Ga_xIn_{1-x}P$ alloys have not been sufficiently explored for improving the device performance for either photovoltaics or solid-state lighting (SSL) although it has been shown that, by increasing the degree of ordering, the alloy fluctuation can indeed be considerably reduced for this alloy system at $x \sim 0.5$.[13] For application in a $Ga_{0.52}In_{0.48}P/GaAs$ two-junction solar cell, ordering actually results in an adverse band-gap lowering. One could have taken advantage of the ordering effect in the recent three- or four-junction solar cell designs, for instance, $Ga_xIn_{1-x}P/GaInAs/Ge$, with x significantly lower than 0.5.[8] However, unfortunately until now, the electronic structure of the ordered phase has been poorly understood for $x \neq 0.5$. For SSL applications, the band-edge emission of $Ga_{0.52}In_{0.48}P$ has been demonstrated to be capable of yielding high internal quantum efficiency at ~650 nm at room temperature (RT). However, to achieve "ultra-efficient" white-light emission in a nonphosphor approach, high internal radiative efficiencies in both the shallow red (615–625 nm) and yellow-green (530–570 nm) spectral regions are needed from primary semiconductors.[9] The commonly adopted route to achieve wavelength tuning is to incorporate Al, forming a quaternary alloy $(Al_yGa_{1-y})_xIn_{1-x}P$. Using this approach, not only is the alloy fluctuation expected to increase further in the quaternary system but also the well-known oxidation effect associated with Al degrades the material quality. The upper limit for $(Al_yGa_{1-y})_{0.51}In_{0.49}P$ on GaAs, determined by the Γ-X direct-to-indirect crossing, corresponds to an energy of ~2.24 eV or an emission wavelength of ~553 nm at RT at $y \sim 0.55$.[43] With the recent improvement in growing $Ga_xIn_{1-x}P$ and $Ga_xIn_{1-x}As$ alloys on a strain-graded buffer layer,[8,44] it is appropriate now to explore the $x > 0.5$ composition region, utilizing the ordering effect to our advantage, for tuning the emission wavelength. The current calculated (0 K) band gap at $x_{\Gamma\text{-}X}$ is 2.333 eV, which implies a RT band gap of ~2.23 eV (assuming the same temperature dependence at $x=0.5$) and sets the upper limit of the direct band gap achievable with $Ga_xIn_{1-x}P$. To target a wavelength within the red gap, 620 nm for instance, we need a 0 K band gap of ~2.1 eV, which can be obtained with $x \sim 0.59$ if disordered or $x \sim 0.7$ if maximally ordered, with the indirect-band edge at least 150–200 meV above the direct band gap. The calculated band gap for $x=0.8$ with maximum ordering is 2.286 eV (with the X-like states 33 meV above), corresponding to a RT band gap of ~2.186 eV (567 nm), which is within the yellow-green band. The same band gap can also be achieved for the disordered phase at $x \sim 0.716$ or for the partially ordered phase with x in between 0.716 and 0.80. By varying x and η, both the transition intensity and the energy separation between the band-edge state and the next indirect critical point could be optimized.

IV. SUMMARY AND CONCLUSIONS

We have performed a systematic study on the effects of alloying and ordering on the electronic and optical properties for random and CuPt-ordered $Ga_xIn_{1-x}P$ alloys using an accurate realistic modeling technique: an improved empirical pseudopotential method in conjunction with the use of very large fully relaxed supercells. For the disordered phase, two long-standing issues are addressed for this alloy system with the following conclusions: (1) the direct-to-indirect crossing point occurs between Γ and X at $x_{\Gamma\text{-}X}=0.75$ and there is only one crossover point and (2) the observation of the zero-phonon absorption and emission associated with the X-like alloy states can be semiquantitatively explained by the calculated transition intensity that reaches a maximum at $x_{\Gamma\text{-}X}$ with a sizable value of 6.6% of that for the direct transition at $x=0.5$. For the CuPt-ordered phase, we have extended the previously well-studied composition $x=0.5$ to x far beyond 0.5. We have predicted (1) the ordering-induced changes in

the fundamental band gap as well as band gaps of higher critical points, (2) the effects of ordering on the optical transition intensity and optical anisotropy, and (3) the interplay of alloying and ordering on the electronic and optical properties. We have provided insights for the relevance of the electronic states in the alloy phase (either in the virtual-crystal approximation or truly random structure) to those in the ordered phase. The accurate electronic structures and optical properties for the disordered and ordered $Ga_xIn_{1-x}P$ alloys will provide valuable guidance for their applications in two important technology areas—photovoltaics and solid-state lighting—and beyond. Additionally, we have shown that because of the atomic displacements due to lattice relaxation, the VCA basis cannot serve as the appropriate zero-order approximation in perturbation calculations for electronic and transport properties of the relaxed alloy.

ACKNOWLEDGMENTS

This work was supported by the DOE-OS-BES under Contracts No. DE-AC36-99GO10337 to NREL and No. DE-AC02-05CH11231 to LBNL. The work used the computational resources of NERSC at LBNL. We thank Suhuai Wei for useful discussions.

*yong_zhang@nrel.gov

[1] M. Bugajski, A. M. Kontkiewicz, and H. Mariette, Phys. Rev. B **28**, 7105 (1983).
[2] Y. Zhang, A. Mascarenhas, and L. W. Wang, Phys. Rev. B **63**, 201312(R) (2001).
[3] M. Altarelli, Solid State Commun. **15**, 1607 (1974).
[4] P. Merle, D. Auvergne, H. Mathieu, and J. Chevalier, Phys. Rev. B **15**, 2032 (1977).
[5] G. D. Pitt, M. K. R. Vyas, and A. W. Mabbitt, Solid State Commun. **14**, 621 (1974).
[6] A. B. Chen and A. Sher, *Semiconductor Alloys, Physics and Materials Engineering* (Plenum, New York, 1995).
[7] H. Mariette, Ph.D. thesis, Universite Pierre et Marie Curie, Paris, 1981.
[8] R. R. King, D. C. Law, K. M. Edmondson, C. M. Fetzer, G. S. Kinsey, H. Yoon, R. A. Sherif, and N. H. Karam, Appl. Phys. Lett. **90**, 183516 (2007).
[9] J. M. Phillips, M. E. Coltrin, M. H. Crawford, A. J. Fischer, M. R. Krames, R. Mueller-Mach, G. O. Mueller, Y. Ohno, L. E. S. Rohwer, J. A. Simmons, and J. Y. Tsao, Laser Photonics Rev. **1**, 307 (2007).
[10] A. Gomyo, T. Suzuki, and S. Iijima, Phys. Rev. Lett. **60**, 2645 (1988).
[11] A. Mascarenhas and Y. Zhang, in *Spontaneous Ordering in Semiconductor Alloys*, edited by A. Mascarenhas (Kluwer Academic, Dordrecht/Plenum, New York, 2002), p. 283.
[12] S.-H. Wei, in *Spontaneous Ordering in Semiconductor Alloys*, edited by A. Mascarenhas (Kluwer Academic, Dordrecht/Plenum, New York, 2002), p. 423.
[13] Y. Zhang, A. Mascarenhas, S. Smith, J. F. Geisz, J. M. Olson, and M. Hanna, Phys. Rev. B **61**, 9910 (2000).
[14] D. B. Laks, S.-H. Wei, and A. Zunger, Phys. Rev. Lett. **69**, 3766 (1992).
[15] M. Kondow, H. Kakibayashi, T. Tanaka, and S. Minagawa, Phys. Rev. Lett. **63**, 884 (1989).
[16] Y. Zhang, A. Mascarenhas, and L.-W. Wang, Phys. Rev. Lett. **101**, 036403 (2008).
[17] S. H. Wei and A. Zunger, Appl. Phys. Lett. **56**, 662 (1990).
[18] Y. Zhang, A. Mascarenhas, and L. W. Wang, Appl. Phys. Lett. **80**, 3111 (2002).
[19] S.-H. Wei and A. Zunger, Appl. Phys. Lett. **53**, 2077 (1988).
[20] R. G. Dandrea and A. Zunger, Appl. Phys. Lett. **57**, 1031 (1990).
[21] K. Yamashita, T. Kita, H. Nakayama, and T. Nishino, Phys. Rev. B **53**, 15713 (1996).
[22] Y. Zhang, A. Mascarenhas, and L. W. Wang, Phys. Rev. B **64**, 125207 (2001).
[23] L.-W. Wang, J. Kim, and A. Zunger, Phys. Rev. B **59**, 5678 (1999).
[24] Y. Zhang, A. Mascarenhas, and L.-W. Wang, Phys. Rev. B **74**, 041201(R) (2006).
[25] P. Keating, Phys. Rev. **145**, 637 (1966).
[26] L. W. Wang and A. Zunger, J. Chem. Phys. **100**, 2394 (1994).
[27] L. Nordheim, Ann. Phys. **9**, 607 (1931).
[28] R. H. Parmenter, Phys. Rev. **97**, 587 (1955).
[29] P. A. Flinn, Phys. Rev. **104**, 350 (1956).
[30] G. L. Hall, Phys. Rev. **116**, 604 (1959).
[31] L. W. Wang, L. Bellaiche, S. H. Wei, and A. Zunger, Phys. Rev. Lett. **80**, 4725 (1998).
[32] K. C. Hass, H. Ehrenreich, and B. Velický, Phys. Rev. B **27**, 1088 (1983).
[33] L. C. Davis, Phys. Rev. B **28**, 6961 (1983).
[34] S.-H. Wei, A. Franceschetti, and A. Zunger, Phys. Rev. B **51**, 13097 (1995).
[35] G. L. Bir and G. E. Pikus, *Symmetry and Strain-Induced Effects in Semiconductors* (Wiley, New York, 1974).
[36] Y. Zhang, Phys. Rev. B **49**, 14352 (1994).
[37] P. H. Tan, X. D. Luo, Z. Y. Xu, Y. Zhang, A. Mascarenhas, H. P. Xin, C. W. tu, and W. K. Ge, Phys. Rev. B **73**, 205205 (2006).
[38] F. Alsina, M. Garriga, M. I. Alonso, J. Pascual, J. Camassel, and R. W. Glew, in Proceedings of the 22nd International Conference in Physics of Semiconductors, edited by D. J. Lockwood (World Scientific, Singapore, 1995), p. 253.
[39] A. N. Pikhtin, Fiz. Tekh. Poluprovodn. (S.-Peterburg) **11**, 425 (1977) [Sov. Phys. Semicond. **11**, 245 (1977)].
[40] M. V. Klein, M. D. Sturge, and E. Cohen, Phys. Rev. B **25**, 4331 (1982).
[41] Y. Zhang, A. Mascarenhas, P. Ernst, F. Driessen, D. J. Friedman, K. A. Bertness, J. M. Olson, C. Geng, F. Scholz, and H. Schweizer, J. Appl. Phys. **81**, 6365 (1997).
[42] J. J. Hopfield, J. Phys. Chem. Solids **15**, 97 (1960).
[43] J. S. Nelson, E. D. Jones, S. M. Myers, D. M. Follstaedt, H. P. Hjalmarson, J. E. Schirber, R. P. Schneider, J. E. Fouquet, V. M. Robbins, and K. W. Carey, Phys. Rev. B **53**, 15893 (1996).
[44] J. F. Geisz, S. Kurtz, M. W. Wanlass, J. S. Ward, A. Duda, D. Friedman, J. M. Olson, W. E. McMahon, T. E. Moriarty, and J. T. Kiehl, Appl. Phys. Lett. **91**, 023502 (2007).